Off-Energy-Shell Behavior of Partial-Wave Scattering Amplitudes*

THOMAS R. MONGAN†
Lawrence Radiation Laboratory, University of California, Berkeley, California 94720
(Received 23 December 1968)

We compare the off-energy-shell behavior of several potential models for the nucleon-nucleon interaction. This is done by comparing the Kowalski-Noyes half-off-shell functions $f_l(p,k)$ resulting from the different models.

I. INTRODUCTION

WE have presented several separable-potential models of the nucleon-nucleon interaction and claimed that these models will be useful in probing the off-energy-shell behavior of the nucleon-nucleon scattering amplitude.[1,2] Therefore, it seems useful to display the off-energy-shell behavior of our models and compare this off-shell behavior with the off-shell behavior produced by some other potential models of the nucleon-nucleon interaction.

The point of the present paper is that the off-energy-shell behavior of separable-potential models is *not* qualitatively different from the off-shell behavior produced by local soft-core Yukawa-potential models. Thus, separable-potential models lead to off-energy-shell scattering amplitudes that are as close to physical reality as the amplitudes resulting from these local potential models. Therefore, at the present state of our knowledge of the nucleon-nucleon interaction, the use of separable-potential models in calculations involving off-energy-shell nucleon-nucleon scattering amplitudes is strongly indicated because of the great convenience and simplicity of the separable-potential models.

If the half-off-energy-shell partial-wave scattering amplitude $T_l(p,k;k^2)$ goes to zero as $k^2\to\infty$, which is true in potential theory, the half-off-shell amplitude is determined by the scattering region ($k^2>0$) values of the on-shell amplitude and the Kowalski-Noyes[3,4] half-off-shell function $f_l(p,k)$, where $f_l(p,k)$ is a *real* function. Similarly, it can be shown that the full off-shell amplitude $T_l(p,p';k^2)$ is determined for all values of k^2 by the scattering region ($k^2>0$) values of the on-shell amplitude and the half-off-shell function $f_l(p,k)$, if $T_l(p,p';k^2)\to 0$ as $k^2\to\infty$.[5] Consequently, in this paper we compare the off-energy-shell behavior of several types of potential models of the nucleon-nucleon interaction by displaying the half-off-shell functions $f_l(p,k)$ for $k^2>0$, generated by the various models.

II. EQUATIONS AND CONVENTIONS

The half-off-shell partial-wave nucleon-nucleon scattering amplitude $T_l(p,k;k^2)$ is determined in potential theory by the two-particle nonrelativistic Lippmann-Schwinger equation

$$T_l(p,k;k^2)=V_l(p,k)+\frac{2\mu}{\hbar^2}\int_0^\infty \frac{q^2dq\,V_l(p,q)T_l(q,k;k^2)}{k^2-q^2+i\epsilon}, \quad (1)$$

where the c.m. kinetic energy $E=\hbar^2k^2/2\mu$, and μ is the reduced mass of the two nucleons.

It can be shown[6] on the basis of time reversal and unitarity alone, that the half-off-shell amplitude $T_l(p,k;k^2)$ can be written

$$T_l(p,k;k^2)=f_l(p,k)T_l(k^2),$$

where $f_l(p,k)$ is a *real* function, and $T_l(k^2)$ is the on-shell partial-wave scattering amplitude

$$T_l(k^2)=-(\hbar^2/\pi\mu k)e^{i\delta_l(k^2)}\sin\delta_l(k^2).$$

In fact, by performing a Fredholm reduction on the singular integral Eq. (1), we can show[3] that the half-off-shell function $f_l(p,k)$ is determined in potential theory by the nonsingular integral equation

$$f_l(p,k)=\frac{V_l(p,k)}{V_l(k,k)}+\frac{2\mu}{\hbar^2}\int_0^\infty\frac{q^2dq}{k^2-q^2}\times\left(V_l(p,q)-\frac{V_l(p,k)V_l(k,q)}{V_l(k,k)}\right)f_l(q,k). \quad (2)$$

The real function $f_l(p,k)$ has the threshold behavior $f_l(p,k)\sim p^l$ as $p\to 0$ and $f_l(p,k)\sim k^{-l}$ as $k\to 0$. Of course, $f_l(k,k)\equiv 1$ and $f_l(p,k)\to\infty$, when $T_l(k^2)\to 0$.

In the separable-potential models we presented earlier, the potential in uncoupled partial waves is

$$V_l(p,p')=g_l(p)g_l(p')-h_l(p)h_l(p'),$$

and the half-off-shell function can be written

$$f_l(p,k)=N_l(p,k)/N_l(k,k), \quad (3)$$

* Work supported in part by the U. S. Atomic Energy Commission.
† Present address: MITRE Corporation, 1820 Dolley Madison Blvd., Westgate Research Park, McLean, Va. 22101.
[1] Thomas R. Mongan, Phys. Rev. **175**, 1260 (1969).
[2] Thomas R. Mongan, Phys. Rev. **178**, 1597 (1969).
[3] K. L. Kowalski, Phys. Rev. Letters **15**, 798 (1965).
[4] H. P. Noyes, Phys. Rev. Letters **15**, 538 (1965).
[5] T. R. Mongan, University of California Radiation Laboratory Report No. UCRL-17452, 1967 (unpublished).
[6] M. I. Sobel, Phys. Rev. **137**, B1517 (1965).

where

$$N_l(p,k)=g_l(p)g_l(k)\left(1+\frac{2\mu}{\hbar^2}P\int_0^\infty\frac{dq\,q^2h_l^2(q)}{k^2-q^2}\right)$$
$$-h_l(p)h_l(k)\left(1-\frac{2\mu}{\hbar^2}P\int_0^\infty\frac{dq\,q^2}{k^2-q^2}g_l^2(q)\right)$$
$$-[g_l(p)h_l(k)+h_l(p)g_l(k)]\frac{2\mu}{\hbar^2}P\int_0^\infty\frac{dq\,q^2}{k^2-q^2}g_l(q)h_l(q),$$

and P indicates a principal-value integral. For a single-term separable potential, we have $V_l(p,p')=\lambda g_l(p)\times g_l(p')$, with $\lambda=\pm1$, and the half-off-shell function is

$$f_l(p,k)=g_l(p)/g_l(k). \tag{4}$$

We have compared the half-off-shell functions in the uncoupled partial waves $^1S_0$, $^1P_1$, and $^1D_2$ resulting from four different separable-potential models of the general form

$$V_l(p,p')=g_l(p)g_l(p')-h_l(p)h_l(p'),$$

and from three different local soft-core Yukawa-potential models of the nucleon-nucleon interaction. These potentials are:

(i) separable-potential case I of Ref. 2 with

$$g_l(p)=G_Rp^l/(p^2+a_R^2)^{(l+1)/2},$$
$$h_l(p)=G_Ap^l/(p^2+a_A^2)^{(l+1)/2}.$$

The potential parameters in the different partial waves are given in Table I;

(ii) separable-potential case II of Ref. 2, with

$$g_l(p)=G_Rp^l/(p^2+a_R^2)^{(l+2)/2},$$
$$h_l(p)=G_Ap^l/(p^2+a_A^2)^{(l+2)/2}.$$

The potential parameters for the different partial waves are displayed in Table I;

(iii) separable-potential case III of Ref. 2 with

$$g_l(p)=\frac{G_Rp^2}{(p^2+\frac{1}{4}\mu_R^2)}\left[\frac{1}{\pi p^2}Q_l\left(1+\frac{\mu_R^2}{2p^2}\right)\right]^{1/2};$$
$$h_l(p)=G_A\left[\frac{1}{\pi p^2}Q_l\left(1+\frac{\mu_A^2}{2p^2}\right)\right]^{1/2},$$

where $Q_l(x)$ is the Legendre function of the second kind and the potential parameters are again given in Table I;

(iv) separable-potential case IV of Ref. 2 with

$$g_l(p)=G_Rp^l/(p^2+a_R^2)^{l+1},$$
$$h_l(p)=G_Ap^l/(p^2+a_A^2)^{l+1}.$$

Note that (iv) is identical to (ii) in the partial wave $^1S_0$. The potential parameters in the different partial waves are entered in Table I;

(v) the local soft-core potential models of Reid.[7] In the partial wave $^1S_0$, the potentials are

$$V_A(x)=-h(e^{-x}/x)-1650.6(e^{-4x}/x)+6484.2(e^{-7x}/x),$$

and

$$V_B(x)=-h(e^{-x}/x)+105.32(e^{-3x}/x)-2401.9(e^{-4x}/x)+5598.2(e^{-6x}/x).$$

In the partial wave $^1P_1$, the potentials are

$$V_A(x)=3h(e^{-x}/x)-634.39(e^{-2x}/x)+2163.4(e^{-3x}/x),$$

or

$$V_B(x)=3h(e^{-x}/x)-240(e^{-2x}/x)+17000(e^{-6x}/x).$$

Finally, in the partial wave $^1D_2$, the potentials are

$$V_A(x)=-h(e^{-x}/x)-318.64(e^{-3x}/x)+526.27(e^{-5x}/x),$$

or

$$V_B(x)=-h(e^{-x}/x)-12.322(e^{-2x}/x)-1112.6(e^{-4x}/x)+6484.2(e^{-7x}/x).$$

In all these potentials, $h=10.463$ MeV and $x=\mu r$, with $\mu=0.7$ F^{-1};

(vi) the local soft-core potential model of Ulehla, Bystricky, and Lehar.[8] In the partial wave $^1S_0$, this

TABLE I. Potential parameters for the separable potentials of Ref. 2.

Partial wave	G_R (MeV F)$^{1/2}$	a_R (F^{-1})	G_A (MeV F)$^{1/2}$	a_A (F^{-1})
		Case I		
$^1S_0$	52.45	2.331	41.36	1.855
$^1P_1$	49.83	1.138	46.16	1.103
$^1D_2$	0.0	···	4.817	1.418
		Case II		
Partial wave	G_R (MeV/F)$^{1/2}$	a_R (F^{-1})	G_A (MeV/F)$^{1/2}$	a_A (F^{-1})
$^1S_0$	302.0	6.157	27.33	1.786
$^1P_1$	40.88	1.410	30.21	1.258
$^1D_2$	0.0	···	21.09	1.944
		Case III		
Partial wave	G_R (MeV F)$^{1/2}$	μ_R (F^{-1})	G_A (MeV F)$^{1/2}$	μ_A (F^{-1})
$^1S_0$	20.84	2.225	10.00	1.300
$^1P_1$	26.53	0.644	31.53	1.256
$^1D_2$	0.0	···	10.61	1.415
		Case IV		
Partial wave	G_R [MeV F$^{-(2l+1)}$]$^{1/2}$	a_R (F^{-1})	G_A [MeV F$^{-(2l+1)}$]$^{1/2}$	a_A (F^{-1})
$^1S_0$	302.0	6.157	27.33	1.786
$^1P_1$	121.6	1.967	49.73	1.566
$^1D_2$	0.0	···	530.5	2.721

[7] Roderick V. Reid, Jr., Center for Theoretical Physics, Laboratory for Nuclear Science, Massachusetts Institute of Technology Report No. CTP-40, 1968 (unpublished).

[8] I. Ulehle, J. Bystricky, and F. Lehar, in *Proceedings of the International Nuclear Physics Conference, Gatlinburg, Tenn., 1966*, edited by R. L. Becker (Academic Press Inc., New York, 1967), p. 687.

TABLE II. Parameters of the soft-core local potentials of Reid and Ulehla *et al.*

$$V_l(p,q)=\sum_{i=1}^{4}\frac{G_i}{\pi pq}Q_l\left(\frac{p^2+q^2+\mu_i^2}{2pq}\right),$$

where the μ_i are in inverse fermis (F^{-1}), and G_i are in MeV F.

Potential	μ_1 (F^{-1})	G_1 (MeV F)	μ_2 (F^{-1})	G_2 (MeV F)	μ_3 (F^{-1})	G_3 (MeV F)	μ_4 (F^{-1})	G_4 (MeV F)
				Partial wave $^1S_0$				
Reid *A*	0.7	−14.947	2.8	−2358.0	4.9	9263.1	···	0.0
Reid *B*	0.7	−14.947	2.1	150.46	2.8	−3431.3	4.2	7497.4
Ulehla *et al.*	0.707	−60.5	1.414	934.0	2.121	−5277.0	2.828	6234.0
				Partial wave $^1P_1$				
Reid *A*	0.7	31.389	1.4	−906.27	2.1	3090.6	···	0.0
Reid *B*	0.7	31.389	1.4	−342.9	4.2	24285.7	···	0.0
Ulehla *et al.*	0.707	−38.5	1.414	359.7	2.121	0.0	2.828	0.0
				Partial wave $^1D_2$				
Reid *A*	0.7	−14.947	2.1	−455.20	3.5	751.81	···	0.0
Reid *B*	0.7	−14.947	1.4	−17.603	2.8	−1589.4	4.4	9263.1
Ulhela *et al.*	0.707	−28.3	1.414	71.0	2.121	5.9	2.828	−1150.0

TABLE III. $^1S_0$ phase shift in degrees generated by different potential models at selected values of the laboratory kinetic energy.

Model \ Lab KE (MeV)	50	100	150	200	250	300	350
Mongan case I	40.0	24.6	14.1	6.2	−0.11	−5.2	−9.6
Mongan case II	40.4	25.0	14.4	6.4	−0.05	−5.4	−10.0
Mongan case III	30.3	16.9	9.1	3.8	−0.06	−3.1	−5.5
Reid *A*	38.6	24.3	14.0	5.8	−1.1	−7.0	−12.2
Reid *B*	38.4	24.1	13.9	5.7	−1.0	−6.8	−11.9
Ulehla *et al.*	39.6	24.9	14.6	6.6	−0.09	−5.4	−10.1
Tabakin single separable	37.0	22.9	13.2	5.4	−1.3	−7.4	−13.0

TABLE IV. $^1P_1$ phase shift in degrees generated by different potential models at selected values of the laboratory kinetic energy.

Model \ Lab KE (MeV)	50	100	150	200	250	300	350
Mongan case I	−3.2	−11.6	−18.2	−23.3	−27.2	−30.3	−32.8
Mongan case II	−2.7	−12.3	−19.7	−24.9	−28.3	−30.6	−32.0
Mongan case III	−3.0	−13.0	−20.0	−24.7	−28.0	−30.3	−32.0
Mongan case IV	−3.6	−12.3	−19.7	−25.3	−29.2	−31.8	−33.3
Reid *A*	−4.3	−11.5	−18.7	−25.2	−30.9	−35.9	−40.4
Reid *B*	−5.5	−11.3	−18.0	−24.6	−30.9	−36.9	−42.4
Ulehla *et al.*	−5.7	−12.3	−17.1	−20.5	−23.2	−25.4	−27.1

potential is

$$V(x)=(m_\pi^2/m_N)[-2.06(e^{-x}/x)+31.8(e^{-2x}/x)-179.6(e^{-3x}/x)+212.2(e^{-4x}/x)],$$

TABLE V. $^1D_2$ phase shift in degrees generated by different potential models at selected values of the laboratory kinetic energy.

Model \ Lab KE (MeV)	50	100	150	200	250	300	350
Mongan case I	1.1	3.3	5.5	7.1	8.4	9.2	9.9
Mongan case II	0.9	3.1	5.4	7.2	8.5	9.3	9.8
Mongan case III	1.4	3.5	5.4	6.9	8.2	9.1	9.9
Mongan case IV	0.8	2.8	5.2	7.2	8.6	9.5	9.8
Reid *A*	1.7	3.6	5.3	6.8	8.0	9.0	9.8
Reid *B*	1.7	3.6	5.4	6.9	8.1	8.9	9.4
Ulehla *et al.*	2.0	3.5	5.2	7.1	9.1	11.3	13.4

while in $^1P_1$, the potential is

$$V(x)=(m_\pi^2/m_N)[-1.31(e^{-x}/x)+12.25(e^{-2x}/x)],$$

and in $^1D_2$, the potential is

$$V(x)=(m_\pi^2/m_N)[-0.962(e^{-x}/x)+2.4(e^{-2x}/x)-0.2(e^{-3x}/x)-39.2(e^{-4x}/x)],$$

where $m_\pi=139.51$ MeV, $m_N=937.0$ MeV and $x=\mu r$, with $\mu=0.707$ F^{-1}.

In momentum space, the potentials of Reid and Ulehla *et al.* are given by

$$V_l(p,q)=\sum_{i=1}^{4}\frac{G_i}{\pi pq}Q_l\left(\frac{p^2+q^2+\mu_i^2}{2pq}\right),$$

where $Q_l(x)$ is the Legendre function of the second kind. The coupling strength G_i and the inverse ranges μ_i in the three cases are given in Table II.

Additionally, in the partial wave $^1S_0$, we consider Tabakin's[9] single-term separable-potential model of the $^1S_0$ interaction. In Tabakin's model

$$V_l(p,p')=g_l(p)g_l(p'), \tag{5}$$

with

$$g_l(p)=\alpha(k_c^2-p^2)[(p^2+d^2)/(p^2+b^2)][1/(p^4+a^4)],$$

where $\alpha^2=400.8434$ F^{-3}, $k_c=1.7$ F^{-1}, $a=4.05$ F^{-1}, $b=1.08548$ F^{-1}, and $d=1.683$ F^{-1}.

III. CALCULATIONS AND RESULTS

First we check the on-shell properties of the different potential models. In Tables III–V, we present the values of the phase shifts generated by the different potential models at selected values of the laboratory kinetic energy.

Next, we obtain the half-off-shell functions $f_l(p,k)$ resulting from our separable-potential models from Eq. (3) and we display $f_l(p,k)$ versus p for fixed values of the laboratory kinetic energy $E_{\rm lab}=2(\hbar^2k^2/2\mu)$ in Figs. 1–8. Note that in the partial wave $^1S_0$ the case II and IV potentials are identical and the case III potential of Ref. 2 has an off-shell behavior substantially different from the other separable-potential models. This behavior is also characteristic of the case I and II fits of Ref. 1, which have specially modified repulsive form factors. The different behavior of $f_l(p,k)$ for large p in the various separable-potential models is clearly displayed in Figs. 5–8.

We now compare the off-shell behavior of our separable-potential models of the nucleon-nucleon inter-

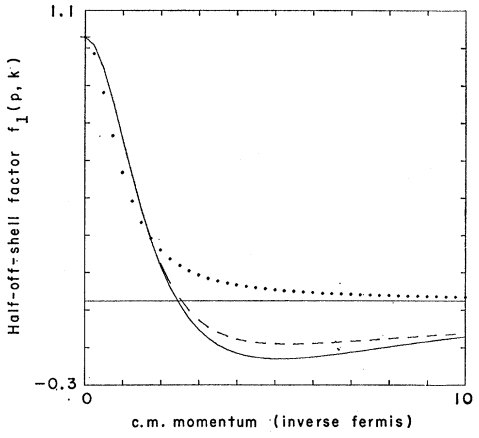

FIG. 1. Noyes-Kowalski half-off-shell functions $f_l(p,k)$ for the separable-potential models of Ref. 2 in the partial wave $^1S_0$ at a lab KE of 0 MeV. The dashed curve represents the case I fit. The solid curve marks the case II and IV fits, which are identical in the partial wave $^1S_0$. The case III fit is indicated by the dotted curve.

[9] F. Tabakin, Phys. Rev. 174, 1208 (1968).

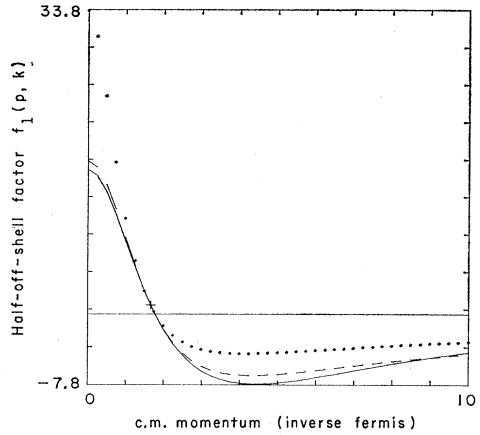

FIG. 2. Noyes-Kowalski half-off-shell functions $f_l(p,k)$ for the separable-potential models of Ref. 2 in the partial wave $^1S_0$ at a lab KE of 230 MeV. Description of the curves is as for Fig. 1.

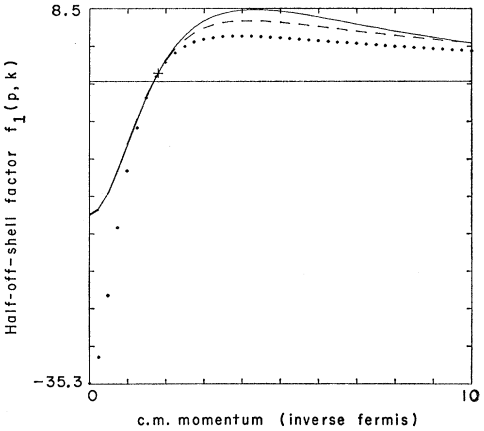

FIG. 3. Noyes-Kowalski half-off-shell functions $f_l(p,k)$ for the separable-potential models of Ref. 2 in the partial wave $^1S_0$ at a lab KE of 270 MeV. Description of the curves is as for Fig. 1.

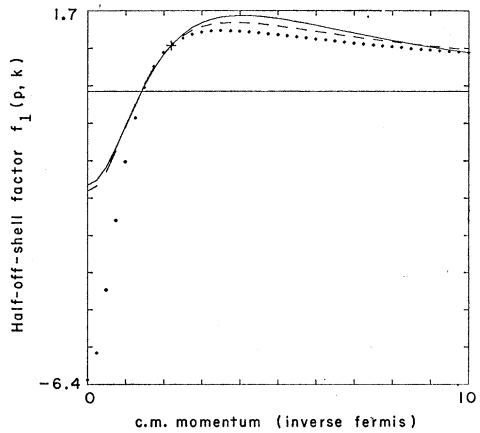

FIG. 4. Noyes-Kowalski half-off-shell functions $f_l(p,k)$ for the separable-potential models of Ref. 2 in the partial wave $^1S_0$ at a lab KE of 400 MeV. Description of the curves is as for Fig. 1.

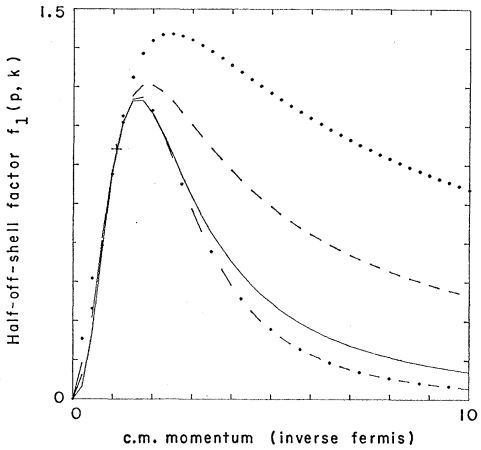

FIG. 5. Noyes-Kowalski half-off-shell functions $f_l(p,k)$ for the separable-potential models of Ref. 2 in the partial wave $^1P_1$ at a lab KE of 100 MeV. The dashed curve represents the case I fit, the solid curve marks the case II fit, the dotted curve indicates the case III fit, and the dot-dash curve denotes the Case IV fit.

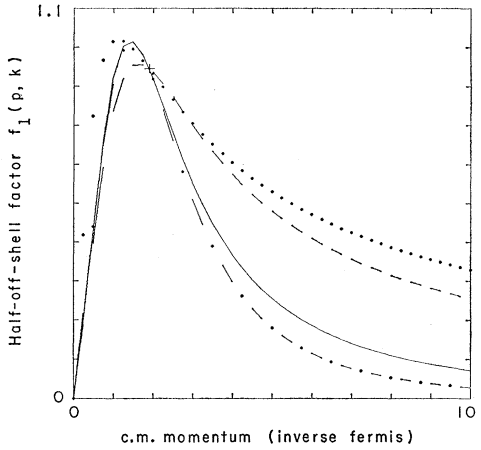

FIG. 6. Noyes-Kowalski half-off-shell functions $f_l(p,k)$ for the separable-potential models of Ref. 2 in the partial wave $^1P_1$ at a lab KE of 300 MeV. Description of the curves is as for Fig. 5.

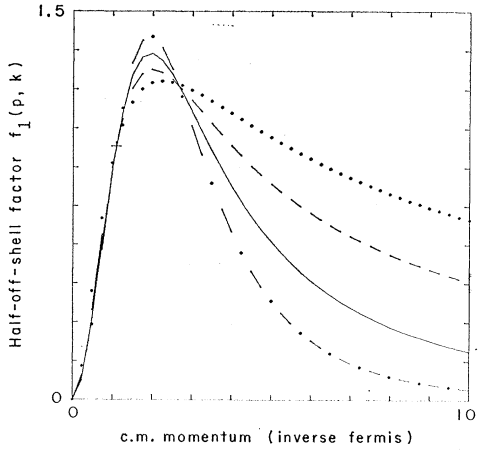

FIG. 7. Noyes-Kowalski half-off-shell functions $f_l(p,k)$ for the separable-potential models of Ref. 2 in the partial wave $^1D_2$ at a lab KE of 100 MeV. Description of the curves is as for Fig. 5.

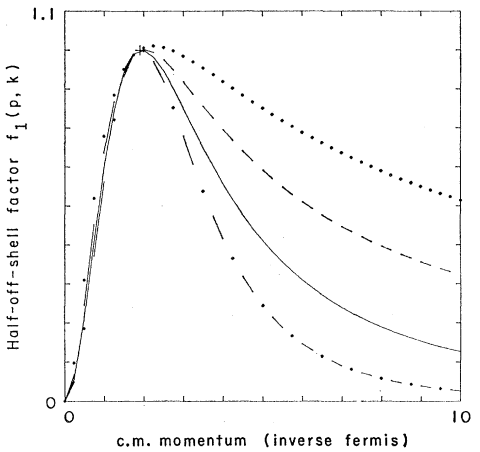

FIG. 8. Noyes-Kowalski half-off-shell functions $f_l(p,k)$ for the separable-potential models of Ref. 2 in the partial wave $^1D_2$ at a lab KE of 300 MeV. Description of the curves is as for Fig. 5.

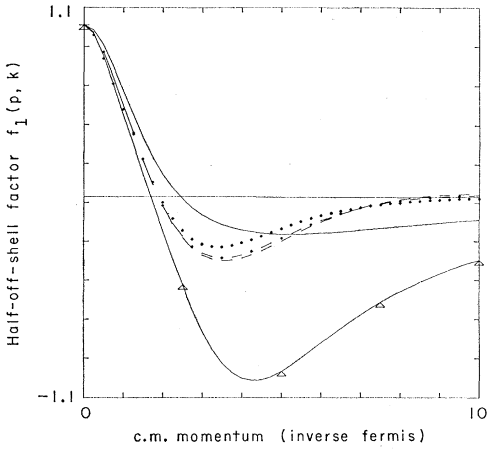

FIG. 9. Comparison of the Noyes-Kowalski half-off-shell functions $f_l(p,k)$ resulting from local-potential models and separable-potential models in the partial wave $^1S_0$ at a lab KE of 0 MeV. The solid curve denotes $f_l(p,k)$ resulting from the separable-potential case II of Ref. 2, which has been chosen as representative of the separable-potential models of Ref. 2. The solid curve marked with Δ represents $f_l(p,k)$ resulting from Tabakin's single-term separable-potential model of the $^1S_0$ interaction. The dotted curve displays $f_l(p,k)$ produced by the local potential model of Ulehla *et al.* The dashed curve indicates $f_l(p,k)$ generated by the local-potential model of Reid which we have called A in the text. The dot-dash curve signifies $f_l(p,k)$ resulting from the local-potential model of Reid which we have called B in the text.

action with the Reid and Ulehla *et al.* local-potential models and Tabakin's separable $^1S_0$ potential. We shall choose case II of Ref. 2 to represent our separable-potential models in this comparison, because it gives the best fit to the on-shell data.

For the local-potential models, $f_l(p,k)$ is obtained by solving the integral Eq. (2) numerically as a matrix inversion problem. For the case II of Ref. 2 separable-potential model, $f_l(p,k)$ is obtained from Eq. (3), while Eq. (4) yields $f_l(p,k)$ for the Tabakin model. We display the results as curves of $f_l(p,k)$ versus p at fixed values of k, in Figs. 9–16.

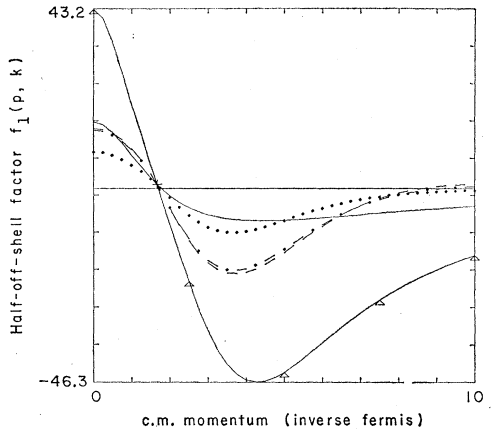

FIG. 10. Comparison of the Noyes-Kowalski half-off-shell functions $f_l(p,k)$ resulting from local-potential models and separable-potential models in the partial wave $^1S_0$ at a lab KE of 230 MeV. Description of the curves is as for Fig. 9.

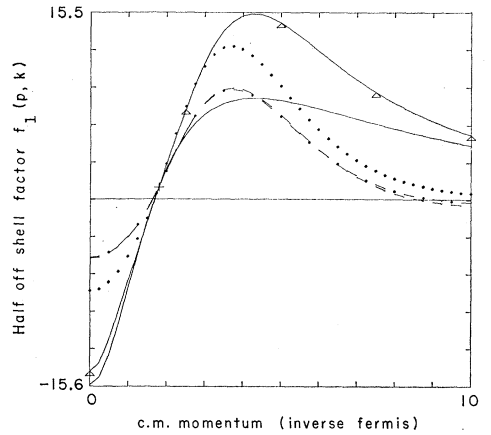

FIG. 11. Comparison of the Noyes-Kowalski half-off-shell functions $f_l(p,k)$ resulting from local-potential models and separable-potential models in the partial wave $^1S_0$ at a lab KE of 270 MeV. Description of the curves is as for Fig. 9.

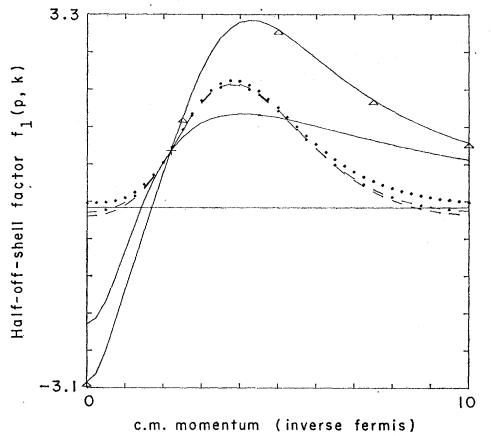

FIG. 12. Comparison of the Noyes-Kowalski half-off-shell functions $f_l(p,k)$ resulting from local-potential models and separable-potential models in the partial wave $^1S_0$ at a lab KE of 400 MeV. Description of the curves is as for Fig. 9.

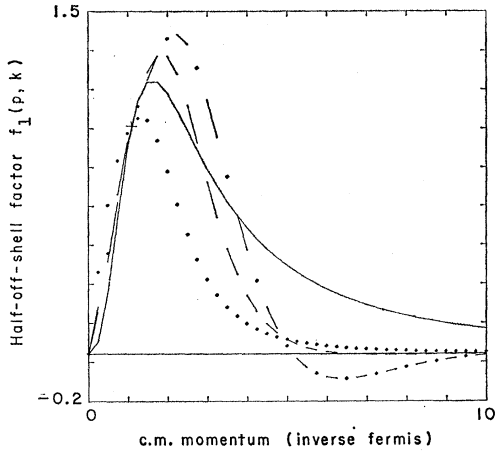

FIG. 13. Comparison of the Noyes-Kowalski half-off-shell functions $f_l(p,k)$ resulting from local-potential models and separable-potential models in the partial wave $^1P_1$ at a lab KE of 100 MeV. The solid curve denotes $f_l(p,k)$ resulting from the separable-potential case II of Ref. 2, which has been chosen as representative of the separable-potential models of Ref. 2. The dotted curve displays $f_l(p,k)$ produced by the local-potential model of Ulehla *et al.* The dashed curve indicates $f_l(p,k)$ generated by the local-potential model of Reid which we have called A in the text. The dot-dash curve signifies $f_l(p,k)$ resulting from the local potential model of Reid which we have called B in the text.

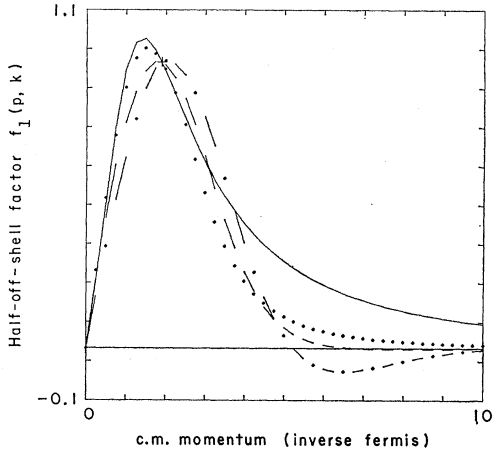

FIG. 14. Comparison of the Noyes-Kowalski half-off-shell functions $f_l(p,k)$ resulting from local-potential models and separable-potential models in the partial wave $^1P_1$ at a lab KE of 300 MeV. Description of the curves is as for Fig. 13.

When we compare the off-shell behavior resulting from the local Yukawa-potential models with the separable-potential models represented by case II of Ref. 2, we find that the off-shell functions in partial waves, with $l=1$ and $l=2$, are quite similar, especially at high energy (i.e., a laboratory kinetic energy of 300 MeV). The agreement would be even better if we had chosen case IV of Ref. 2 to represent our separable-potential models, because the case IV potentials lead to an asymptotic behavior

$$f_l(p,k)\sim 1/p^{l+2} \quad \text{as } p\to\infty\,,$$

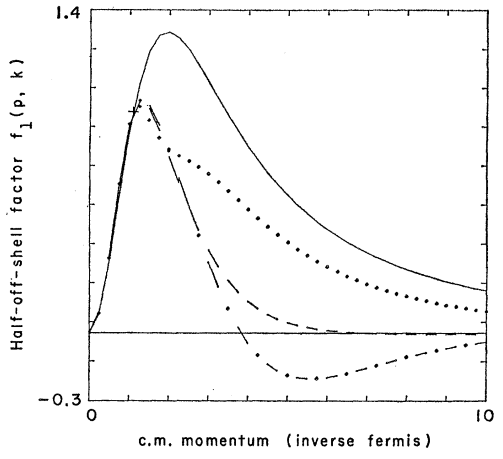

FIG. 15. Comparison of the Noyes-Kowalski half-off-shell functions $f_l(p,k)$ resulting from local-potential models and separable-potential models in the partial wave $^1D_2$ at a lab KE of 100 MeV. Description of the curves is as for Fig. 13.

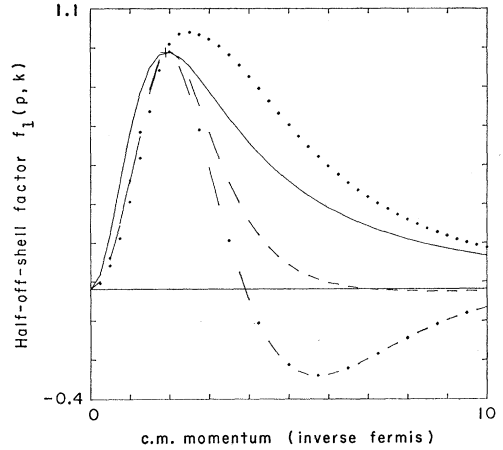

FIG. 16. Comparison of the Noyes-Kowalski half-off-shell functions $f_l(p,k)$ resulting from local-potential models and separable-potential models in the partial wave $^1D_2$ at a lab KE of 300 MeV. Description of the curves is as for Fig. 13.

which is the same as the asymptotic behavior resulting from a superposition of Yukawa potentials. Correspondingly, the agreement of the off-shell functions resulting from the local Yukawa models with the off-shell functions generated by the separable model is somewhat worse in cases I and III.

The greatest difference between the off-shell functions resulting from the local potentials and our separable-potential models is in the partial wave $^1S_0$ at a laboratory kinetic energy of 400 MeV and momentum $p=0$, where $f_l(p,k)\approx 0$ for the local-potential models and $f_l(p,k)$ is of order 1 for the separable models. Also, in the partial wave $^1S_0$, the function $f_l(p,k)$ produced by our separable-potential models falls off more slowly as $p\rightarrow\infty$ than the off-shell functions resulting from the local-potential models. Notice that the single separable-potential model of the $^1S_0$ interaction given by Tabakin seems to lead to an off-shell function somewhat different from those produced by other models.

Our contention that the off-energy-shell behavior of separable-potential models is not in contradiction with experiment and is not drastically different in a calculational sense from the off-shell behavior produced by local potentials is borne out, respectively, by the success of Tabakin's earlier separable-potential model of the nucleon-nucleon interaction in nuclear physics calculations[10] and by the agreement of the separable-potential p-p bremsstrahlung calculation of Pearce, Gale, and Duck,[11] with the local-potential calculations and with experiment.

Our results have been checked by utilizing programs which solve the Lippmann-Schwinger Eq. (1) as a complex matrix inversion problem to obtain the amplitudes $T_l(p,k;k^2)$ and $T_l(k^2)$. These amplitudes determine $f_l(p,k)$ by the equation $f_l(p,k)=T_l(p,k,k^2)/T_l(k^2)$, and this result is checked against $f_l(p,k)$ calculated from Eqs. (2) and (3).

IV. COMMENTS AND CONCLUSIONS

We would first like to remark on Tabakin's[9] single-separable-potential model of the $^1S_0$ nucleon-nucleon interaction as set forth in Eq. (5). This model leads to a pole in the full off-energy-shell amplitude $T_l(p,p';k^2)$ at $k^2=k_c^2$, which does not occur in the actual full off-shell amplitude.[5] If the Tabakin model is used in three-body scattering calculations, this spurious singularity or "positive-energy bound state," as Tabakin calls it, will lead to cuts in the three-body scattering amplitudes similar to those resulting from the scattering of a free particle off a real physical bound state of the other two.[12] It is difficult to predict the effects or assess the physical significance of these somewhat artificial cuts. Although the Tabakin potential yields an off-shell function $f_l(p,k)$ that is rather different from the off-shell functions resulting from our separable-potential models or from the local soft-core Yukawa-potential models, we believe that the Tabakin potential may provide a useful model for the off-shell function $f_l(p,k)$. If the Tabakin model is used only to generate the off-shell function $f_l(p,k)$, the half-off-shell scattering amplitude may be written $T_l(p,k;k^2)=\alpha_l(p)\beta_l(k)T_l(k^2)$, with $T_l(k^2)$ written in terms of the experimental phase shifts and $\alpha_l(p)$ and $\beta_l(k)$ obtained directly from the Tabakin model. Additionally, a separable model of the off-shell factor $f_l(p,k)$ in the form $f_l(p,k)=\alpha_l(p)\beta_l(k)$ is very useful when studying the full off-shell amplitude.[5]

It seems that the necessity of fitting the on-shell data constrains our separable-potential models and the

[10] F. Tabakin, Ann. Phys. (N.Y.) **30**, 51 (1964).
[11] W. A. Pearce, W. A. Gale, and I. M. Duck, Nucl. Phys. **B3**, 241 (1967).
[12] C. Lovelace, Phys. Rev. **135**, B1225 (1964).

local soft-core Yukawa potentials to share the same qualitative off-shell behavior. This is not surprising in view of the smoothness of the mathematical forms of the potentials.

Our separable-potential models do show some variation in off-shell behavior, especially for large values of p in $f_l(p,k)$. This reinforces our hopes that the use, in calculations involving the off-energy-shell two-body scattering amplitude, of the form

$$T_l(p,p';k^2)=F_l(p,p';k^2)T_l(k^2),$$

with $F_l(p,p';k^2)$ determined by the separable-potential models and $T_l(k^2)$ written in terms of the experimental phase shifts, will enable us to discern the sensitivity of these calculations to the off-energy-shell behavior of the amplitudes.

We have demonstrated that separable-potential models lead to an off-energy-shell behavior, which is *not* qualitatively different from the off-shell behavior resulting from local soft-core Yukawa-potential models of the nucleon-nucleon interaction. Since separable-potential models do not produce any freakish effects off the energy shell, they seem to have an equally valid claim to presenting a realistic representation of the off-shell nucleon-nucleon interaction as the local-potential models. Therefore, since the separable-potential models are so much simpler, their use in calculations involving the off-energy-shell nucleon-nucleon partial-wave scattering amplitude is strongly indicated.

PHYSICAL REVIEW VOLUME 180, NUMBER 5 25 APRIL 1969

Effect of Weak Interactions on Electromagnetic Properties of Leptons*

S. Rai Choudhury and H. S. Mani
Physics Department, University of Michigan, Ann Arbor, Michigan 48104
(Received 5 December 1968)

We have investigated the electromagnetic properties of leptons in the presence of weak interactions, using a model essentially similar to the one recently developed by Gell-Mann, Goldberger, Kroll, and Low. We find that the effect is very small in the anomalous magnetic moment and in the Lamb shift of hydrogen. However, the charge radius of the neutrino turns out to be much larger than the previous estimate of Bernstein and Lee.

I. INTRODUCTION

RECENT investigations in the theory of weak interactions have brought to surface the fact that the conventional $(V-A)$ theory, with or without the intermediate vector boson, runs into serious difficulties, once it is regarded as a full-fledged field theory. The origin of these difficulties lies in the nonrenormalizability of the theory, with the result that one cannot subtract away the infinities arising out of integration of the internal momenta in a higher-order diagram. However, the first-order results are not divergent and are in good agreement with experimental data at low energies. In trying to get rid of the divergence difficulties without essentially disturbing the first-order low-energy results, one assumes that the basic interaction somehow gets cut off or damped out at high energies and high virtual momenta, thus providing the required convergence to make all higher-order graphs finite. Now, the energy at which the first-order theory must necessarily fail is the energy at which it starts violating unitarity, and in the absence of anything more suggestive, it is natural to use this as the cutoff value in the internal-momenta integrations. The resulting cutoff value Λ_u turns out to be $\sqrt{(1/G)}$,[1] where G is the Fermi coupling constant. However, its use in the conventional theory leads to serious conflicts with experiments since it then predicts strong violation of strong selection rules and far too large an amplitude for second-order weak processes like $K^0\to\mu^+\mu^-$. In a recent paper, Gell-Mann, Goldberger, Kroll, and Low[2] have proposed a modification of the conventional theory which bypasses these difficulties. In their model the hadronic current interacts not only with an intermediate vector boson but also with a set of scalar and pseudoscalar mesons and the various interactions are so arranged such that if one uses the cutoff Λ_u in internal-momenta integrations one has no disagreements with experimental facts at the order-of-magnitude level. In this note we investigate, in a theory of this type, the effect of weak interactions on the electromagnetic properties of leptons.

In Sec. II, we present a simplified version of the GGKL model which contains all the essential aspects of their basic idea. In Sec. III, we introduce electromagnetic interactions and evaluate the electromagnetic prop-

* Research supported in part by AFOSR under Grant No. 1288-67.

[1] Λ^2 is the value of the formally divergent integral $(2\pi)^{-4}\int d^4q/q^2$, after it has been regularized. With this definition, the expansion fails for $G\Lambda^2\sim 1$, which can be considered as the definition of the unitarity cutoff.